

Wavelet Galerkin method in multi-scale homogenization of heterogeneous media

Shafiq Mehraeen and Jiun-Shyan Chen^{*,†}

Department of Civil and Environmental Engineering, University of California, Los Angeles 5713 Boelter Hall, Los Angeles, CA 90095-1593, U.S.A.

SUMMARY

The hierarchical properties of scaling functions and wavelets can be utilized as effective means for multi-scale homogenization of heterogeneous materials under Galerkin framework. It is shown in this work, however, when the scaling functions are used as the shape functions in the multi-scale wavelet Galerkin approximation, the linear dependency in the scaling functions renders improper zero energy modes in the discrete differential operator (stiffness matrix) if integration by parts is invoked in the Galerkin weak form. An effort is made to obtain the analytical expression of the improper zero energy modes in the wavelet Galerkin differential operator, and the improper nullity of the discrete differential operator is then removed by an eigenvalue shifting approach. A unique property of multi-scale wavelet Galerkin approximation is that the discrete differential operator at any scale can be effectively obtained. This property is particularly useful in problems where the multi-scale solution cannot be obtained simply by a wavelet projection of the finest scale solution without utilizing the multi-scale discrete differential operator, for example, the multi-scale analysis of an eigenvalue problem with oscillating coefficients. Copyright © 2005 John Wiley & Sons, Ltd.

KEY WORDS: multi-scale; wavelet; Galerkin method; homogenization; heterogeneous

1. INTRODUCTION

There is an increasing demand of using compound and composite materials for complicated systems. Homogenization methods have been developed to analyse how these materials behave in different conditions. Homogenization is a collection of methods for extracting or constructing equations for the coarse scale behaviour of materials and systems, which incorporate many scales. The objective of homogenization is to construct simpler fine scale equations, which are considerably less expensive to solve, and whose solutions have the same coarse scale properties

*Correspondence to: Jiun-Shyan Chen, Professor, Department of Civil and Environmental Engineering, University of California, Los Angeles, 5731G Boelter Hall, Los Angeles, CA 90095-1593, U.S.A.

†E-mail: jschen@seas.ucla.edu

Contract/grant sponsor: NSF; contract/grant number: CMS 0084589

Received 17 June 2004

Revised 18 October 2004

Accepted 17 August 2005

as the solutions of the complicated systems. The classical theory of homogenization was given by Bensoussan *et al.* [1]. Homogenized Dirichlet projection method [2, 3] was developed based on the concept of hierarchical modelling. In this method, the mathematical model at the coarsest level is represented by homogenized material properties. Error estimate has been developed for identifying the error between the coarse scale solution using homogenized properties and the fine scale solution of the heterogeneous material with microstructures [2]. In the sub-domain with larger error, a local boundary value problem is solved. This approach was further extended to a hierarchical modelling of heterogeneous materials where the most essential scales of the problem can be adaptively selected in the discretization [3].

In the asymptotic expansion approach [1], the relationship between the macroscopic and microscopic solution can be derived, and the corresponding homogenized differential operator and homogenized coefficients for solving the macroscopic solution can be obtained. Alternatively, a multi-grid method for a periodic heterogeneous medium has been introduced [4, 5]. In this approach, a multi-grid method is employed to develop a fast iterative solver for differential equations with oscillatory coefficients. An intergrid transfer operator is constructed following the asymptotic expansion so that the problem on the auxiliary grid gives rise to a homogenization problem. The limitation of the two above-mentioned methods is that they necessitate the fine scale response of the material to be fairly separated from the response on the coarser scales.

In the recent multi-resolution approach given in References [6, 7], an equation for the coarse scale component of the solution can be directly constructed. Utilizing the notion of the multi-resolution analysis (MRA), the relation between two different scales is explicitly defined. This process is based on the reduction (static condensation) procedure, which involves computing the Schur complement of fine scale. The reduction procedure can be repeated over several scales, and thus it does not require the small parameter assumptions, which are typical for asymptotic methods [8]. Knapik [4] has applied Schur complement for a multi-grid-based homogenization technique. Multi-resolution strategy using wavelet functions for homogenization has been applied to system of linear ordinary differential equations [6]. MRA constructed based on wavelet-like reproducing kernel approximation has been presented [9, 10]. In Reference [11] the wavelet-based projection method was proposed by introducing wavelet functions as basis for multi-scale homogenization of an elasticity problem with oscillatory coefficients.

The wavelet Galerkin method entails representing the solution as expansion of scaling functions at a particular scale, and one chooses both test and trial functions to be wavelet basis functions. The solution to the differential equation is therefore approximated by a truncated wavelet expansion, with the advantage that the multi-resolution and localization properties of wavelets can be exploited. The choice of wavelet basis is governed by several factors including the desired order of numerical accuracy, computational effort and other constraints such as scale decomposition. Compactly supported wavelets of Daubechies have been applied to solve differential equations under the framework of wavelet Galerkin method [12–16]. Compact wavelets perform well in resolving high gradients, and they can be used for adaptive refinement. The higher-order derivatives of scaling functions and wavelets in the wavelet Galerkin method are usually highly oscillatory and thus are difficult to integrate. Further, standard wavelet Galerkin formulation is constructed by a direct multiplication of strong form with wavelet basis functions that leads to an asymmetric discrete system. Although exact method of integration for wavelet and scaling function has been developed [17], this method is confined to the orthogonal compactly supported wavelets of Daubechies.

In this work, a set of scaling function and wavelet based on the linear hat function are employed as the basis functions. An integration by parts is introduced to the weak form to reduce the order of differentiation and to yield a symmetric discrete system, and natural boundary conditions are invoked in the weak form. However, due to the use of the translation rule of scaling functions, the dependency of shape functions in this approach renders a singular stiffness matrix if integration by parts is invoked in the weak form. This problem is resolved by shifting improper zero eigenvalues. It is demonstrated that the proposed wavelet Galerkin method provides a hierarchical representation of the homogenized solution at different scales. Subsequently, the multi-resolution properties of the wavelet functions are exploited to smoothen the inhomogeneity in the multi-scale solution of the differential equation.

The content of this chapter is catalogued as follows. In Section 2, the basic properties of scaling function and wavelet are reviewed. In Section 3, symmetrized wavelet Galerkin method using scaling function and wavelet based on the linear hat function is introduced, and the cause and remedy of singularity in the stiffness matrix is discussed. In Section 4, wavelet Galerkin method in multi-scale homogenization is presented. Several numerical examples are given to demonstrate and validate the proposed method in Section 5. Concluding remarks are outlined in Section 6.

2. WAVELET SPACES

To establish the hierarchical approximation of functions in the proposed multi-scale homogenization, the scaling functions and wavelet spaces are first reviewed in this section [18]. The hierarchical scaling functions are constructed by first defining a nested sequence of closed subspace $\{V_j\}_{j \in \mathbb{Z}}$ with the properties: $\dots \subset V_{-1} \subset V_0 \subset V_1 \subset \dots \subset L^2(R)$, $\bigcup_{j \in \mathbb{Z}} V_j = L^2(R)$, and $\bigcap_{j \in \mathbb{Z}} V_j = \{0\}$. Each subspace is spanned by a set of scaling functions $V_j = \text{span}\{\phi_{j,n}(x) = 2^{j/2}\phi(2^j x - n)\}$, where $\phi(x)$ is a candidate function. Each subspace V_j is related to its next finer level subspace V_{j+1} by requiring that if $\phi_{j,n}(x) \in V_j$, then $\phi_{j,n}(2x) \in V_{j+1}$. Further, the translates of $\phi(x)$ span the same subspace, i.e. if $\phi_{j,n}(x) \in V_j$, $\phi_{j,n+k}(x) \in V_j$ for any $n, k \in \mathbb{Z}$. The following piecewise constant function and linear function (hat function) are examples of the candidate function:

$$\text{Haar: } \phi(x) = \begin{cases} -1 & -1 \leq x \leq 0 \\ 1 & 0 < x \leq 1 \\ 0 & \text{otherwise,} \end{cases} \quad \text{Linear: } \phi(x) = \begin{cases} 1+x & -1 \leq x \leq 0 \\ 1-x & 0 < x \leq 1 \\ 0 & \text{otherwise} \end{cases} \quad (1)$$

Any function in V_j can be expressed in terms of the basis functions of V_{j+1} , $\phi_{j,k}(x) = \sum_{n=-\infty}^{\infty} a_n \phi_{j+1,n}$. For Haar and linear systems, these two-scale relations are:

$$\text{Haar: } \phi(x) = \phi(2x - 1) + \phi(2x), \quad \text{Linear: } \phi(x) = \frac{1}{2}\phi(2x - 1) + \phi(2x) + \frac{1}{2}\phi(2x + 1) \quad (2)$$

For a given subspace V_j , an orthonormal complement subspace W_j can be defined so that $V_j = V_{j-1} \oplus W_{j-1}$. The subspace W_j is called the wavelet space and is spanned by another orthonormal basis $W_j = \text{span}\{\psi_{j,n}(x) = 2^{j/2}\psi(2^j x - n)\}$, where the mother wavelet $\psi(x)$ can

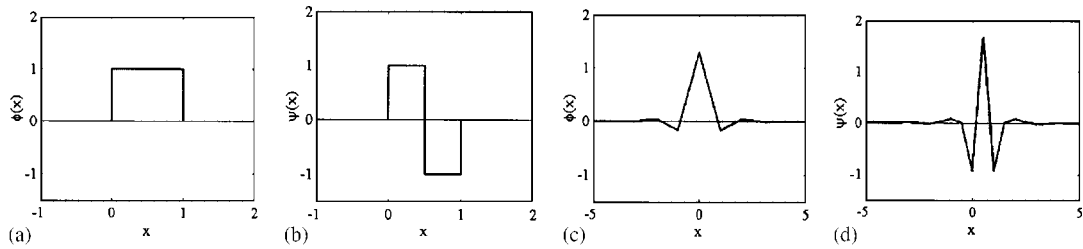


Figure 1. (a) Haar scaling function; (b) corresponding wavelet; (c) linear orthogonal scaling function; and (d) corresponding wavelet.

be expressed in terms of the scaling candidate function $\phi(x)$ by $\psi(x) = \sum_{n=-\infty}^{\infty} b_n \phi(2x - n)$. The important features in the wavelet transformation are the orthogonality conditions between scale functions and wavelets. For a given candidate function $\phi(x)$, a set of orthonormal scaling functions in translation $\phi^*(x)$ can be constructed by imposing the orthogonality conditions $\phi_{j,k}^*(x) = \sum_n \alpha_n \phi_{j,n+k}$ using Parseval identity. By virtue of $W_{j-1} \oplus V_{j-1} = V_j$, orthogonal wavelet function can be expressed as $\psi_{j,k}^*(x) = \sum_m \beta_m \phi_{j+1,m+2k}$ in which coefficients β_m are obtained from orthogonality conditions.

In 2D, the nested subspaces are defined as $\mathbf{V}_j = V_j \otimes V_j$, where \mathbf{V}_j and V_j are the scaling function spaces in 2D and 1D, respectively. Operator \otimes denotes the tensor product in the multi-dimensional space. Consequently, \mathbf{V}_j is spanned by the 2D scaling function basis $\phi_{j,m}^* \otimes \phi_{j,n}^*(x, y)$ where $\phi_{j,m}^*(x)$ is the corresponding 1D scaling function. For a given \mathbf{V}_j , the orthonormal complement subspace \mathbf{W}_{j-1} is defined by $\mathbf{W}_j = (V_j \otimes W_j) \oplus (W_j \otimes V_j) \oplus (W_j \otimes W_j)$. The Haar system and linear orthogonal scaling function and associated wavelet are shown in Figure 1. The 2D linear orthogonal scaling functions and wavelets are shown in Figure 2.

3. MULTI-SCALE WAVELET GALERKIN DISCRETE EQUATION

We will introduce scaling functions and wavelets as the multi-scale shape functions in the approximation of weak form. Note that in this construction of discrete equations, no periodicity assumption is needed.

3.1. Wavelet discrete equation

Without loss of generality, consider the following heterogeneous boundary value problem in 1D

$$\frac{d}{dx} \left(E(x) \frac{du}{dx} \right) + b = 0 \quad \text{on } \Omega \quad (3)$$

$$u = g \quad \text{on } \partial\Omega \quad (4)$$

where for elasticity b is the body force and $E(x)$ is the heterogeneous Young's modulus which in general is a function of x -co-ordinate. In order to reduce the order of differentiation and to

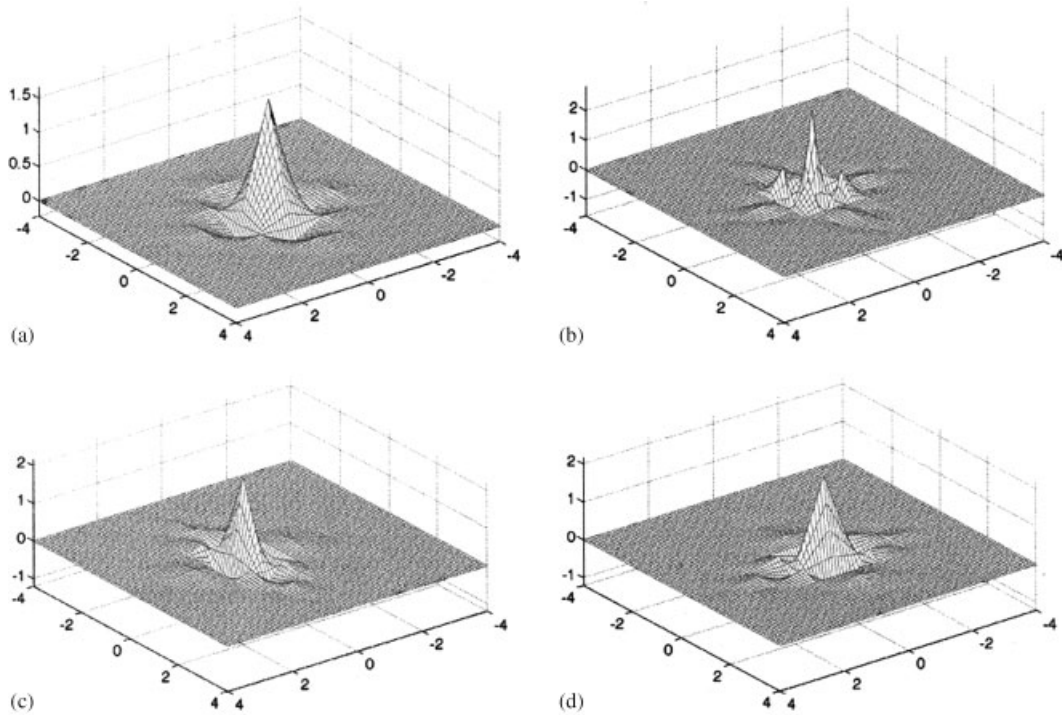


Figure 2. (a) 2D linear orthogonal scaling function in $V_j \otimes V_j$, and three components of wavelet functions in; (b) $V_j \otimes W_j$; (c) $W_j \otimes V_j$; and (d) $W_j \otimes W_j$.

yield a symmetric discrete differential operator, an integration by parts procedure is invoked in the construction of weak form to yield

$$\int_{\Omega} \frac{d\delta u}{dx} E(x) \frac{du}{dx} dx - \int_{\Omega} \delta u b dx + \lambda \delta u|_{\partial\Omega} + \delta \lambda (u|_{\partial\Omega} - g) = 0 \tag{5}$$

where λ is Lagrange multiplier to impose Dirichlet boundary conditions. The approximated solution $u(x)$ at scale $j + 1$ in the solution space V_{j+1} , $u^{j+1}(x)$, is expressed by

$$u^{j+1}(x) = \bar{u}^j(x) + \tilde{u}^j(x) = \boldsymbol{\phi}^j \mathbf{U}^j \tag{6}$$

where $\bar{u}^j(x)$ and $\tilde{u}^j(x)$ are coarse and fine scale components of the solution of scale j approximated by scaling and wavelet basis functions, respectively

$$\bar{u}^j(x) = \sum_k \bar{u}_k^j \phi_{j,k}^*(x) = \boldsymbol{\phi}^j \bar{\mathbf{U}}^j \tag{7}$$

$$\tilde{u}^j(x) = \sum_k \tilde{u}_k^j \psi_{j,k}^*(x) = \boldsymbol{\psi}^j \tilde{\mathbf{U}}^j \tag{8}$$

where

$$\mathbf{U}^j = \begin{bmatrix} \bar{\mathbf{U}}^j \\ \tilde{\mathbf{U}}^j \end{bmatrix}, \quad \bar{\mathbf{U}}^{jT} = [\bar{u}_m^j \ \bar{u}_{m+1}^j \ \cdots \ \bar{u}_{n-1}^j \ \bar{u}_n^j], \quad (9)$$

$$\begin{aligned} \tilde{\mathbf{U}}^{jT} &= [\tilde{u}_m^j \ \tilde{u}_{m+1}^j \ \cdots \ \tilde{u}_{n-1}^j \ \tilde{u}_n^j] \\ \boldsymbol{\varphi} &= [\boldsymbol{\phi}^{j*} \ \boldsymbol{\psi}^{j*}], \quad \boldsymbol{\phi}^{j*} = [\phi_{j,m}^* \ \phi_{j,m+1}^* \ \cdots \ \phi_{j,n-1}^* \ \phi_{j,n}^*], \\ \boldsymbol{\psi}^{j*} &= [\psi_{j,m}^* \ \psi_{j,m+1}^* \ \cdots \ \psi_{j,n-1}^* \ \psi_{j,n}^*] \end{aligned} \quad (10)$$

Here m and n are lower and upper limits of integer translation for orthogonal scaling functions and wavelets. Introducing scale decomposition Equation (6) into Equation (5), we obtain the following scale-decomposed discrete equation.

$$\begin{bmatrix} \bar{\mathbf{K}}^j & \widehat{\mathbf{K}}^j \\ \widehat{\mathbf{K}}^{jT} & \tilde{\mathbf{K}}^j & \boldsymbol{\varphi}^T|_{\partial\Omega} \\ & \boldsymbol{\varphi}|_{\partial\Omega} & 0 \end{bmatrix} \begin{bmatrix} \bar{\mathbf{U}}^j \\ \tilde{\mathbf{U}}^j \\ \lambda \end{bmatrix} = \begin{bmatrix} \bar{\mathbf{F}}^j \\ \tilde{\mathbf{F}}^j \\ g \end{bmatrix} \quad (11)$$

where the scale-decomposed stiffness matrices and force vectors are

$$\bar{\mathbf{K}}^j = \int_{\Omega} \frac{d\boldsymbol{\phi}^{j*T}}{dx} E(x) \frac{d\boldsymbol{\phi}^{j*}}{dx} dx, \quad \widehat{\mathbf{K}}^j = \int_{\Omega} \frac{d\boldsymbol{\phi}^{j*T}}{dx} E(x) \frac{d\boldsymbol{\psi}^{j*}}{dx} dx, \quad (12)$$

$$\tilde{\mathbf{K}}^j = \int_{\Omega} \frac{d\boldsymbol{\psi}^{j*T}}{dx} E(x) \frac{d\boldsymbol{\psi}^{j*}}{dx} dx$$

$$\bar{\mathbf{F}}^j = \int_{\Omega} \boldsymbol{\phi}^{j*T} b dx, \quad \tilde{\mathbf{F}}^j = \int_{\Omega} \boldsymbol{\psi}^{j*T} b dx \quad (13)$$

Upon solving coarse- and fine-scale components of the solution from Equation (11), the lower-scale solutions can be obtained by the wavelet up-sampling using the following two-scale relationship:

$$\phi_{j,l}^* = \sum_k [a_{l-2k} \phi_{j-1,k}^* + b_{l-2k} \psi_{j-1,k}^*] \quad (14)$$

where a_{l-2k} and b_{l-2k} are obtained from the two-scale relations between orthogonal scaling functions and wavelets. Consequently the fine and coarse components of the $j-1$ scale solution (down-sampling) is calculated by

$$\bar{u}_k^{j-1} = \sum_l a_{l-2k} \bar{u}_l^j, \quad \tilde{u}_k^{j-1} = \sum_l b_{l-2k} \tilde{u}_l^j \quad (15)$$

By repeating this wavelet transformation to the lower-scales, the homogenized solution is obtained.

Conversely, an up-sampling of solution can be achieved by the reconstruction (coarse to fine) relationship

$$\phi_{j,n}^* = \sum_k r_k \phi_{j+1,k+2n}^*, \quad \psi_{j,n}^* = \sum_k s_k \phi_{j+1,k+2n}^* \tag{16}$$

where r_k are s_k are obtained from the two-scale relations between orthogonal scaling functions and wavelets. With above coarse and fine scale relationships in the basis functions, the coarse-scale solution of scale $j + 1$ can be obtained from the coarse- and fine-scale solutions of scale j

$$\bar{u}_k^{j+1} = \sum_l [r_{k-2l} \bar{u}_l^j + s_{k-2l} \tilde{u}_l^j] \tag{17}$$

3.2. Singularity in the wavelet discrete equation

Due to the C^0 continuity in the linear scaling functions and wavelets, employment of these basis functions in the Galerkin approximation requires integration by parts of the weak form. It will be shown in the following discussion, however, that the resulting discrete equation of the wavelet Galerkin method is in fact singular due to the dependency of the basis functions at any sub-domain between two given discrete points. If linear orthogonal scaling functions and wavelets are employed as the basis functions, any interval between two discrete points $\Omega_{(i)} = [x_i, x_{i+1}]$ is covered by six linear functions as illustrated in Figures 3(a)–(c), and they are linearly dependent. How this linear dependency in the basis functions at any sub-domain $\Omega_{(i)} = [x_i, x_{i+1}]$ results in the singularity of stiffness matrix is investigated below, and a method to resolve stiffness matrix singularity is also proposed.

Consider the following internal energy at scale- j :

$$\frac{1}{2} \int_{\Omega} E(x) (\bar{u}_{,x}^j)^2 dx = \sum_i \frac{1}{2} \int_{\Omega_{(i)}} E(x) (\bar{u}_{(i),x}^j)^2 dx \tag{18}$$

where $\Omega_{(i)} = [x_i, x_{i+1}]$, and \bar{u}^j in the sub-domain $\Omega_{(i)}$, denoted as $\bar{u}_{(i)}^j$, is approximated by six scaling functions (Figure 3(c)) as

$$\bar{u}_{(i)}^j(x) = \sum_{m=0}^5 \bar{u}_{i-2+m}^j \phi_{j,i-2+m}^*(x) \tag{19}$$

Since $\phi_{j,i-2+m}^*(x)$ in $\Omega_{(i)} = [x_i, x_{i+1}]$ is a linear function, it can be expressed as

$$\phi_{j,i-2+m}^*(x) = p_m x + q_m \tag{20}$$

and thus $\bar{u}_{(i)}^j$ is approximated as

$$\bar{u}_{(i)}^j(x) = \sum_{m=0}^5 \bar{u}_{i-2+m}^j (p_m x + q_m) \tag{21}$$

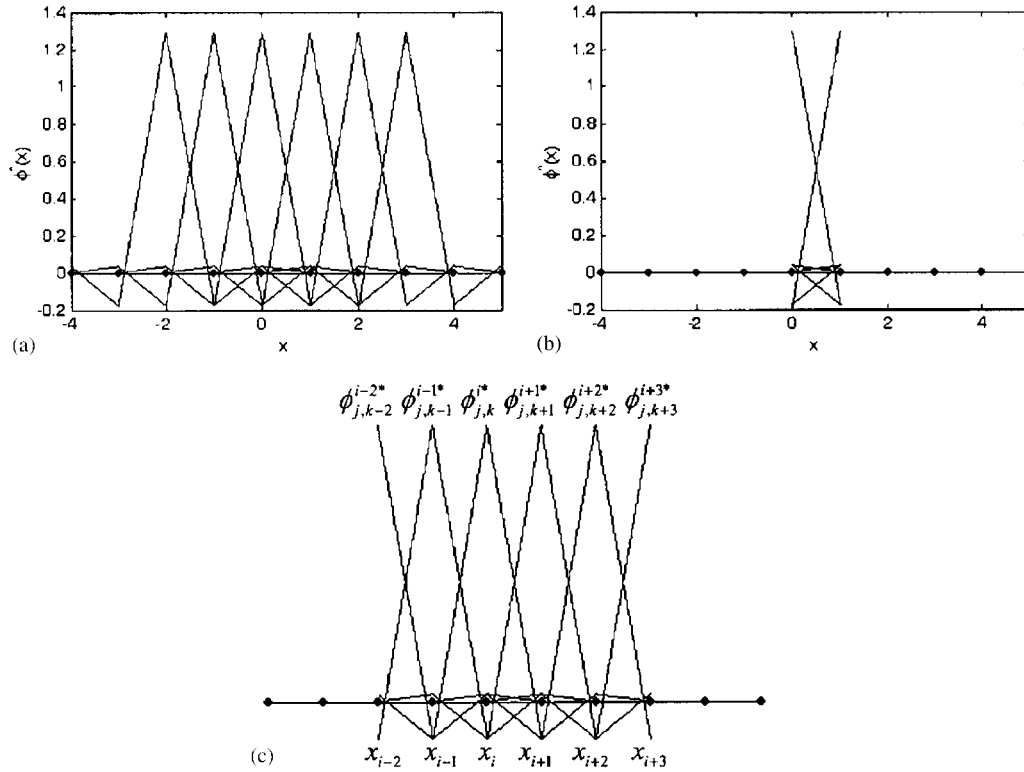


Figure 3. (a) Translation of scaling function; (b) dependency of shape functions between two discrete points; and (c) shape functions contributed to element stiffness matrix.

The derivative of $\bar{u}_{(i)}^j$ is obtained as

$$\bar{u}_{(i),x}^j(x) = \sum_{m=0}^5 \bar{u}_{i-2+m}^j p_m = \mathbf{B}\bar{\mathbf{u}}_{(i)}^j \quad (22)$$

where

$$\mathbf{B} = [p_0, p_1, p_2, p_3, p_4, p_5], \quad \bar{\mathbf{u}}_{(i)}^{jT} = [\bar{u}_{i-2}^j, \bar{u}_{i-1}^j, \bar{u}_i^j, \bar{u}_{i+1}^j, \bar{u}_{i+2}^j, \bar{u}_{i+3}^j] \quad (23)$$

Using symmetries of the basis functions we have $p_3 = -p_2, p_4 = -p_1, p_5 = -p_0$, and thus

$$\mathbf{B} = [p_0, p_1, p_2, -p_2, -p_1, -p_0] \quad (24)$$

and the corresponding scale- j stiffness matrix associated with sub-domain $\Omega_{(i)}$ is

$$\mathbf{K}_{(i)}^j = \int_{\Omega_{(i)}} E(x) \mathbf{B}^T \mathbf{B} \, d\Omega \quad (25)$$

The rank of the gradient matrix \mathbf{B} in Equation (24) reveals that the stiffness $\mathbf{K}_{(i)}^j$ associated with $\frac{1}{2} \int_{\Omega_i} E(x) (\bar{u}_{(i),x}^j)^2 dx$ has a rank of 1, and consequently a nullity of 5. Our next task is to obtain the basis vectors that span the null space of $\mathbf{K}_{(i)}^j$. The necessary condition for $\frac{1}{2} \int_{\Omega_i} E(x) (\bar{u}_{(i),x}^j)^2 dx = 0$ is $\bar{u}_{(i),x}^j = 0$, i.e.

$$\mathbf{B}\bar{\mathbf{u}}_{(i)}^j = 0 \tag{26}$$

Further using the decomposition coefficients given in Table AI (Appendix A) reveals $p_1 = -5.9606p_0$, $p_1 = 41.6454p_0$. Thus, Equation (26) yields

$$\bar{u}_{i-2}^j = \xi \bar{u}_{i-1}^j - \eta \bar{u}_i^j + \eta 4 \bar{u}_{i+1}^j - \xi \bar{u}_{i+2}^j + \bar{u}_{i+3}^j, \quad \xi = 5.9606, \quad \eta = 41.6454 \tag{27}$$

Any vector $\bar{\mathbf{u}}_{(i)}^j$ with components satisfying Equation (26) is in the null space of $\mathbf{K}_{(i)}^j$ (also called the zero energy modes in elasticity), and can be expressed as

$$\bar{\mathbf{u}}_{(i)}^j = \begin{bmatrix} \bar{u}_{i-2}^j \\ \bar{u}_{i-1}^j \\ \bar{u}_i^j \\ \bar{u}_{i+1}^j \\ \bar{u}_{i+2}^j \\ \bar{u}_{i+3}^j \end{bmatrix} = \bar{u}_{i-1}^j \mathbf{r}_1 + \bar{u}_i^j \mathbf{r}_2 + \bar{u}_{i+1}^j \mathbf{r}_3 + \bar{u}_{i+2}^j \mathbf{r}_4 + \bar{u}_{i+3}^j \mathbf{r}_5 \tag{28}$$

$$\mathbf{r}_1 = \begin{bmatrix} \xi \\ 1 \\ 0 \\ 0 \\ 0 \\ 0 \end{bmatrix}, \quad \mathbf{r}_2 = \begin{bmatrix} -\eta \\ 0 \\ 1 \\ 0 \\ 0 \\ 0 \end{bmatrix}, \quad \mathbf{r}_3 = \begin{bmatrix} \eta \\ 0 \\ 0 \\ 1 \\ 0 \\ 0 \end{bmatrix}, \quad \mathbf{r}_4 = \begin{bmatrix} -\xi \\ 0 \\ 0 \\ 0 \\ 1 \\ 0 \end{bmatrix}, \quad \mathbf{r}_5 = \begin{bmatrix} 1 \\ 0 \\ 0 \\ 0 \\ 0 \\ 1 \end{bmatrix} \tag{29}$$

Since $\{\mathbf{r}_1, \mathbf{r}_2, \mathbf{r}_3, \mathbf{r}_4, \mathbf{r}_5\}$ are linearly independent, they can be employed as the five basis vectors that span the null space of $\mathbf{K}_{(i)}^j$.

Note that $\{\mathbf{r}_1, \mathbf{r}_2, \mathbf{r}_3, \mathbf{r}_4, \mathbf{r}_5\}$ are local zero energy modes associated with $\frac{1}{2} \int_{\Omega_i} E(x) (\bar{u}_{(i),x}^j)^2 dx$, and thus they are not necessarily commutable in the global system associated with $\frac{1}{2} \int_{\Omega} E(x) (\bar{u}_{(i),x}^j)^2 dx = \sum_i \frac{1}{2} \int_{\Omega_i} E(x) (\bar{u}_{(i),x}^j)^2 dx$. For a vector in the null space of $\mathbf{K}_{(i)}^j$ to be globally

commutable, it has to take the following form:

$$\begin{bmatrix} \bar{u}_{i-1}^j \\ \bar{u}_i^j \\ \bar{u}_{i+1}^j \\ \bar{u}_{i+2}^j \\ \bar{u}_{i+3}^j \end{bmatrix} = \alpha \begin{bmatrix} \bar{u}_{i-2}^j \\ \bar{u}_{i-1}^j \\ \bar{u}_i^j \\ \bar{u}_{i+1}^j \\ \bar{u}_{i+2}^j \end{bmatrix} \quad (30)$$

For condition in Equation (30) to hold we have used the property that scaling of any vector in the null space belongs to the same null space. Equation (30) yields

$$\bar{u}_{i+3}^j = \alpha \bar{u}_{i+2}^j = \alpha^2 \bar{u}_{i+1}^j = \alpha^3 \bar{u}_i^j = \alpha^4 \bar{u}_{i-1}^j = \alpha^5 \bar{u}_{i-2}^j \quad (31)$$

Thus the commutable local zero energy mode associated with the sub-domain $\Omega_{(i)}$ must take the form $[1, \alpha, \alpha^2, \alpha^3, \alpha^4, \alpha^5]^T$. This yields

$$\begin{bmatrix} 1 \\ \alpha \\ \alpha^2 \\ \alpha^3 \\ \alpha^4 \\ \alpha^5 \end{bmatrix} = \bar{u}_{i-1}^j \mathbf{r}_1 + \bar{u}_i^j \mathbf{r}_2 + \bar{u}_{i+1}^j \mathbf{r}_3 + \bar{u}_{i+2}^j \mathbf{r}_4 + \bar{u}_{i+3}^j \mathbf{r}_5 \quad (32)$$

This leads to a set of equations to find the coefficients $\{\bar{u}_{i-1}^j, \bar{u}_i^j, \bar{u}_{i+1}^j, \bar{u}_{i+2}^j, \bar{u}_{i+3}^j\}$ and α :

$$\begin{bmatrix} \xi & -\eta & \eta & -\zeta & 1 \\ 1 & 0 & 0 & 0 & 0 \\ 0 & 1 & 0 & 0 & 0 \\ 0 & 0 & 1 & 0 & 0 \\ 0 & 0 & 0 & 1 & 0 \\ 0 & 0 & 0 & 0 & 1 \end{bmatrix} \begin{bmatrix} \bar{u}_{i-1}^j \\ \bar{u}_i^j \\ \bar{u}_{i+1}^j \\ \bar{u}_{i+2}^j \\ \bar{u}_{i+3}^j \end{bmatrix} = \begin{bmatrix} 1 \\ \alpha \\ \alpha^2 \\ \alpha^3 \\ \alpha^4 \\ \alpha^5 \end{bmatrix} \quad (33)$$

Solving above system by utilizing the last five equations and substituting the solution into the first equation in Equation (33) yields the following constrain equation for α

$$\xi\alpha - \eta\alpha^2 + \eta\alpha^3 - \zeta\alpha^4 + \alpha^5 - 1 = 0 \quad (34)$$

Solution to Equation (34) is

$$\begin{aligned} \alpha_1 &= 1 \\ \alpha_{2,3} &= 2.4133 \pm 5.4942i \\ \alpha_{4,5} &= 0.0670 \pm 0.1526i \end{aligned} \tag{35}$$

in which $i = \sqrt{-1}$. Above analysis yields five global zero energy modes, denoted as \mathbf{z}_m , as follows:

$$\mathbf{z}_1 = [1, 1, \dots, 1]^T, \quad \mathbf{z}_m = [1, \alpha_m, \alpha_m^2, \dots, \alpha_m^n]^T, \quad m = 2 \sim 5 \tag{36}$$

The first zero energy mode $\mathbf{z}_1 = [1, 1, \dots, 1]^T$ is a physical rigid body mode. This zero energy mode can be removed with imposition of essential boundary conditions. The other four zero energy modes $\mathbf{z}_m, m = 2 \sim 5$ are complex. Note that the real-valued zero energy modes can be obtained as

$$\mathbf{w}_2 = \frac{1}{2}(\mathbf{z}_2 + \mathbf{z}_3), \quad \mathbf{w}_3 = \frac{1}{2i}(\mathbf{z}_2 - \mathbf{z}_3), \quad \mathbf{w}_4 = \frac{1}{2}(\mathbf{z}_4 + \mathbf{z}_5), \quad \mathbf{w}_5 = \frac{1}{2i}(\mathbf{z}_4 - \mathbf{z}_5) \tag{37}$$

These four improper zero energy modes are due to the dependency of the linear scaling basis functions and need to be suppressed for the discrete equation of Equation (3) to be solvable. The singularity in the scale- j global stiffness matrix \mathbf{K}^j can be removed without affecting the physical solution of the original problem if the force vector associated with the differential equation is in the range of the stiffness matrix. Following Chen *et al.* [19], the improper zero eigenvalue in the discrete equation can be shifted to a non-zero value without affecting the non-zero eigenvalues and the corresponding eigenvectors by the following modification of the stiffness matrix:

$$\mathbf{K}^{j*} = \mathbf{K}^j + \sum_{m=2}^5 \varepsilon_m \mathbf{w}_m^T \mathbf{w}_m, \quad \varepsilon_m \neq 0 \tag{38}$$

An eigenvector expansion analysis can be employed to show that the solution of the discrete equation using \mathbf{K}^{j*} will retain the physical solution of the original discrete equation, and the non-physical part of the solution due to the improper nullity of \mathbf{K}^j is suppressed.

4. WAVELET GALERKIN MULTI-SCALE HOMOGENIZATION

The wavelet transformation is defined to transform functions in different scales

$$w_j : V_{j+1} \rightarrow V_j \oplus W_j \tag{39}$$

where w_j is an orthogonal operator which maps the basis $\{\varphi_{j+1,k}^*\}$ onto $\{\varphi_{j,k}^*, \psi_{j,k}^*\}$. We denote the L_2 -projection onto V_j and W_j by operators \mathbf{P}_j and \mathbf{Q}_j such that

$$\begin{aligned} \mathbf{P}_j &: V_{j+1} \rightarrow V_j \\ \mathbf{Q}_j &: V_{j+1} \rightarrow W_j \end{aligned} \tag{40}$$

Now, let \mathbf{w}_j be the transformation matrix that decomposes solution \mathbf{U}_{j+1} into $\tilde{\mathbf{U}}_{j+1}$ and $\bar{\mathbf{U}}_{j+1}$, fine and coarse scale components, respectively. Using the discrete transformation operators \mathbf{P}_j and \mathbf{Q}_j for scaling function and wavelet, respectively, the transformation matrix \mathbf{w}_j takes the form of

$$\mathbf{w}_j = \begin{bmatrix} \mathbf{Q}_j \\ \mathbf{P}_j \end{bmatrix} \tag{41}$$

and

$$\mathbf{w}_j \mathbf{U}_{j+1} = \begin{bmatrix} \mathbf{Q}_j \\ \mathbf{P}_j \end{bmatrix} \mathbf{U}_{j+1} = \begin{bmatrix} \tilde{\mathbf{U}}_{j+1} \\ \bar{\mathbf{U}}_{j+1} \end{bmatrix} \tag{42}$$

Let the discrete boundary value problem in Equation (11) (after applying static condensation to remove the Lagrange multipliers) be expressed by

$$\mathbf{L}\mathbf{U} = \mathbf{F} \tag{43}$$

where \mathbf{L} is the discrete differential operator associated with the weak form. This discrete equation on the space V_{j+1} is

$$\mathbf{L}_{j+1} \mathbf{U}_{j+1} = \mathbf{F}_{j+1} \tag{44}$$

where operator \mathbf{L}_{j+1} acts on the space V_{j+1} . By taking the hierarchical property of scaling function and wavelet as shape functions, the coarse-fine scale decomposition can be utilized via performing the transformation of Equation (41)

$$(\mathbf{w}_j \mathbf{L}_{j+1} \mathbf{w}_j^{-1})(\mathbf{w}_j \mathbf{U}_{j+1}) = \begin{bmatrix} \mathbf{L}_{11} & \mathbf{L}_{12} \\ \mathbf{L}_{21} & \mathbf{L}_{22} \end{bmatrix} \begin{bmatrix} \tilde{\mathbf{U}}_{j+1} \\ \bar{\mathbf{U}}_{j+1} \end{bmatrix} = \mathbf{w}_j \mathbf{F}_{j+1} = \begin{bmatrix} \tilde{\mathbf{F}}_{j+1} \\ \bar{\mathbf{F}}_{j+1} \end{bmatrix} \tag{45}$$

where $\tilde{\mathbf{F}}_{j+1}$ and $\bar{\mathbf{F}}_{j+1}$ denote the fine and coarse scale components of \mathbf{F}_{j+1} , respectively. Here, the discrete transformation matrix \mathbf{w}_j in Equation (42) is constructed by combining operators \mathbf{P}_j and \mathbf{Q}_j . \mathbf{P}_j and \mathbf{Q}_j for the linear orthogonal scaling function and wavelet are written in the matrix form as

$$\mathbf{P}_j = \begin{bmatrix} a_{j-2k} & 0 & 0 & 0 & 0 & \dots & 0 & 0 & 0 \\ a_{j-2(k+1)} & a_{j+1-2(k+1)} & a_{j+2-2(k+1)} & 0 & 0 & \dots & 0 & 0 & 0 \\ a_{j-2(k+2)} & a_{j+1-2(k+2)} & a_{j+2-2(k+2)} & a_{j+3-2(k+2)} & a_{j+4-2(k+2)} & \dots & 0 & 0 & 0 \\ \vdots & \vdots & \vdots & \vdots & \vdots & \vdots & \vdots & \vdots & \vdots \\ 0 & 0 & 0 & 0 & 0 & \dots & a_{j+m-2-2(k+n-1)} & a_{j+m-1-2(k+n-1)} & a_{j+m-2(k+n-1)} \\ 0 & 0 & 0 & 0 & 0 & \dots & 0 & 0 & a_{j+m-2(k+n)} \end{bmatrix} \tag{46}$$

$$\mathbf{Q}_j = \begin{bmatrix}
 b_{j-2k} & 0 & 0 & 0 & 0 & \dots & 0 & 0 & 0 \\
 b_{j-2(k+1)} & b_{j+1-2(k+1)} & b_{j+2-2(k+1)} & 0 & 0 & \dots & 0 & 0 & 0 \\
 b_{j-2(k+2)} & b_{j+1-2(k+2)} & b_{j+2-2(k+2)} & b_{j+3-2(k+2)} & b_{j+4-2(k+2)} & \dots & 0 & 0 & 0 \\
 \vdots & \vdots & \vdots & \vdots & \vdots & \vdots & \vdots & \vdots & \vdots \\
 0 & 0 & 0 & 0 & 0 & \dots & b_{j+m-2-2(k+n-1)} & b_{j+m-1-2(k+n-1)} & b_{j+m-2(k+n-1)} \\
 0 & 0 & 0 & 0 & 0 & \dots & 0 & 0 & b_{j+m-2(k+n)}
 \end{bmatrix} \tag{47}$$

where k , n , and m are specified from the non-zero decomposition coefficients of the sequence a_i and b_i . Decomposition coefficients a_i and b_i , tabulated in Table AI in Appendix A, are obtained by means of z transform of scaling function and wavelet in Equation (14) [18].

The coarsened solution $\bar{\mathbf{U}}_{j+1}$ in Equation (45) is obtained by solving the Schur complement of \mathbf{L}_{11} as

$$[\mathbf{L}_{22} - \mathbf{L}_{21}\mathbf{L}_{11}^{-1}\mathbf{L}_{12}]\bar{\mathbf{U}}_{j+1} = \bar{\mathbf{F}}_{j+1} - \mathbf{L}_{21}\mathbf{L}_{11}^{-1}\tilde{\mathbf{F}}_{j+1} \tag{48}$$

Computing transformation matrix \mathbf{w}_j for coarser levels and repeating above static condensation, we can obtain hierarchy of discretized differential operator at all levels whose solutions are coarse scale solution at those levels. Note that to reach the coarsened solution at a specific level, one constructs discretized differential operator at the finest scale, coarsen it to the desired level, and only solve it once at the level.

Similarly, by applying two scale relations in Equation (16), the reconstruction algorithm as stated in Equation (17) can be utilized. The above-mentioned wavelet Galerkin method in homogenization is applicable to 2D problems summarized in Appendix B.

Remarks

Compared to the multi-scale finite element method proposed by Christon *et al.* [20], the employment of orthogonality between the coarse- and fine-scale components of solutions in the proposed method offers a faster zoom-in and zoom-out operations in multi-scale homogenization and localization. It is also shown in the aforementioned discussion that the discrete differential operator at any scale can be obtained simply by a wavelet transformation if the finest scale discrete differential operator is constructed using scaling functions. Other methods such as the one presented in Reference [11] only allows the transformation of solution to different scales, and it does not provide the mechanism to obtain the multi-scale discrete differential operators that are needed in problems such as eigenvalue analysis of heterogeneous materials, as will be shown in Section 5.2.

5. NUMERICAL EXAMPLES

5.1. Multi-scale homogenization in one dimension

Consider the following elasticity model problem

$$\begin{aligned}
 \frac{d}{dx} \left(E(x) \frac{du(x)}{dx} \right) &= 0, \quad x \in]0, 5[\\
 u(0) &= -5, \quad u'(5) = 1
 \end{aligned} \tag{49}$$

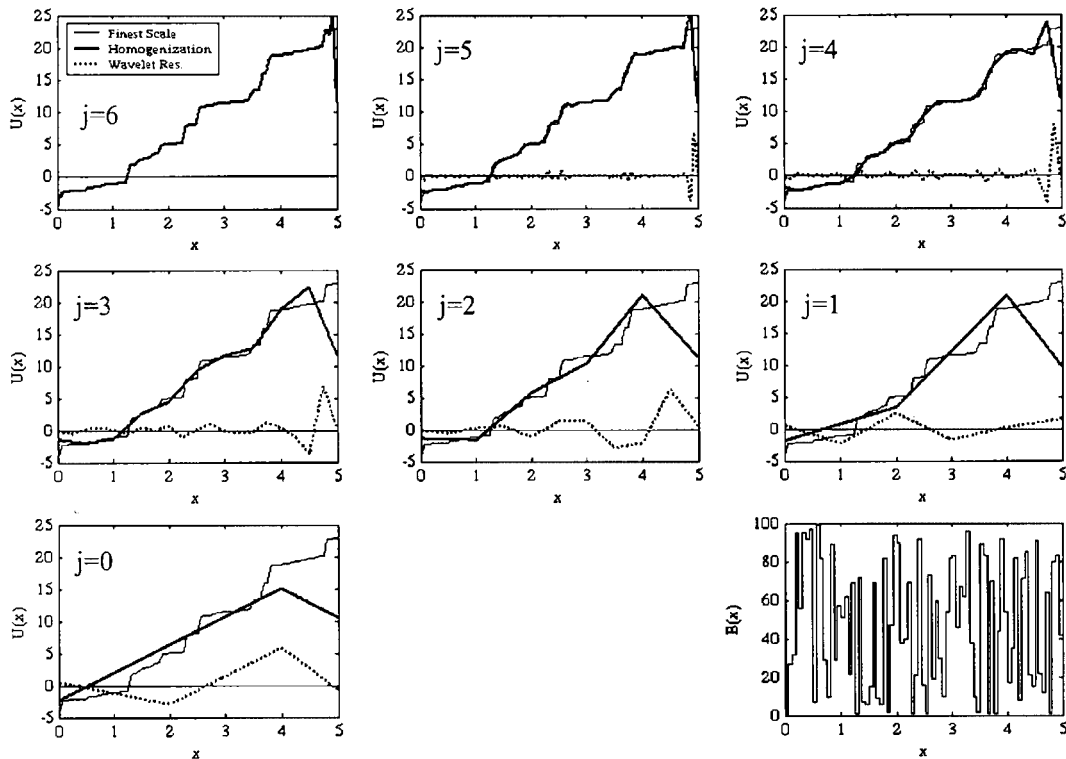


Figure 4. Multi-scale wavelet Galerkin homogenization without using mirror image technique (j : level of resolution, $(E(x)u'(x))' = 0$, $u(0) = -5$, $u'(5) = 1$).

Here we consider the fictitious domain to be $\Omega' = \{x \mid x \in]-5, 10[\}$. A highly oscillating coefficient $E(x)$ as shown in Figure 4 is introduced. Employing shifting eigenvalue method, we shift zero eigenvalues to unity. To capture the fine scale details of the solution, the finest grid associated with the finest scale of the solution is set at $j = 6$. We employ linear orthogonal scaling function and wavelet as illustrated in Figures 1(c) and (d) as the shape functions, since the Haar basis cannot be applied in the wavelet Galerkin method due to its nature of discontinuity. Moreover, the mirror image method as summarized in Appendix C must be employed to have an accurate representation of the solution at the boundaries in the homogenization process. In the following discussion, analysis with and without the mirror image technique are compared.

Homogenization starts from the fine scale $j = 6$ as shown in Figure 4. Without the use of the mirror image technique, boundary conditions cannot be accurately preserved, and oscillations are observed. This is a result of the participation of unknown information associated with the external shape functions that extend beyond the real domain of the problem. As homogenization proceeds, the oscillation initiated near the boundaries at the finer scales propagates to the interior of the problem domain at the coarser scales.

In the second case, the mirror image technique is employed. It is clearly shown in Figure 5 that the oscillation is completely removed and a much more enhanced solution is obtained.

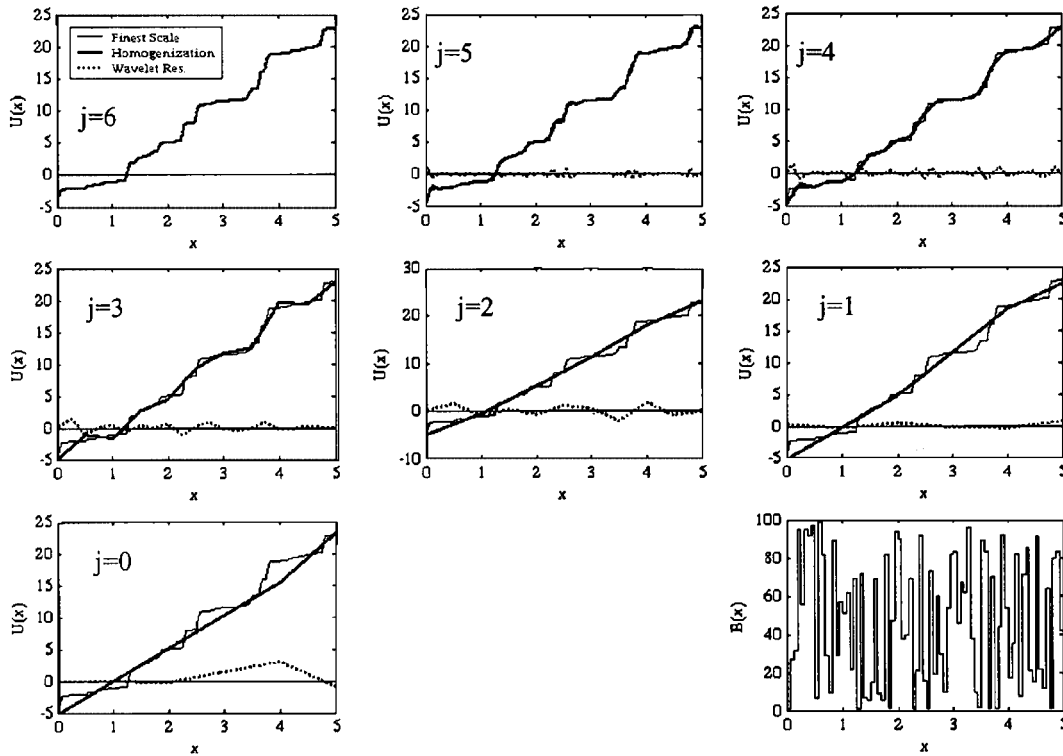


Figure 5. Multi-scale wavelet Galerkin homogenization with mirror image technique (j : level of resolution, $(E(x)u'(x))' = 0$, $u(0) = -5$, $u'(5) = 1$).

The homogenization process is carried out in seven levels. In each level the number of grid points is decreased by half. The finest scale solution is filtered out step by step through the homogenization process, which corresponds to the reduction of degrees of freedom (DOF) in the discrete system. At the coarsest scale $j = 0$, the homogenized solution yields a constant Young's modulus.

We also examine the proposed method when the Dirichlet boundary conditions $u(0) = -20$, $u(5) = 20$ are specified as shown in Figure 6. It can be seen that unlike the asymptotic method, the multi-scale wavelet-based homogenization method is applicable even if the material property is not periodic.

5.2. Multi-scale eigenvalue problems

The essence of wavelet Galerkin multi-scale homogenization is that it allows the transformation of the solution in different scales using multi-scale discrete differential operators. These discrete differential operators at different scales describe the governing equations of the transformed field variables at those scales. This is the main advantage over the method presented in Reference [11] in which the mechanism to obtain the multi-scale discrete differential operators cannot be

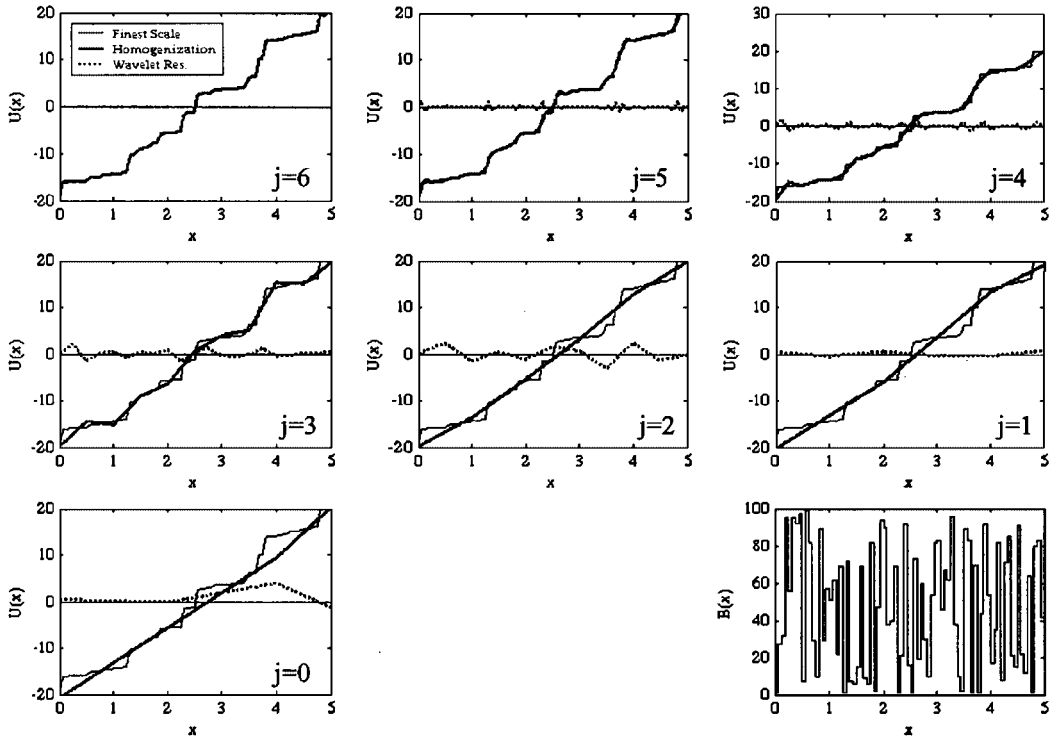


Figure 6. Multi-scale wavelet Galerkin homogenization for $(E(x)u'(x))' = 0$, $u(0) = -20$, $u(5) = 20$ using linear orthogonal scaling function and wavelet enhanced by mirror image technique.

obtained. To demonstrate, consider the following eigenvalue problem

$$\frac{d}{dx} \left(E(x) \frac{du(x)}{dx} \right) + \beta u(x) = 0, \quad x \in]0, 10[\tag{50}$$

$$u(0) = \frac{du}{dx}(10) = 0$$

where β and $u(x)$ are eigenvalue and eigenfunction, respectively. Here, $E(x)$ is an oscillatory coefficient as shown in Figure 7. To capture all the details in the finest eigenfunctions, Equation (11) is used to compute the discrete differential operator at the finest scale $j = 9$. After utilizing static condensation to remove the Lagrange multiplier in Equation (11), we perform operator decomposition scheme described in Section 4 to yield homogenized discrete operator of the coarse level. This procedure is carried out to arrive at the coarse scale ($j = 3$) discrete equation. Comparison of the first six eigenfunctions at scales $j = 9$ and $j = 3$ obtained from the proposed multi-scale wavelet Galerkin method is illustrated in Figure 8. It is obvious that homogenization identity is inherited to the eigenfunctions of lower scales as we compute homogenized operators at multiple scales using the hierarchical property embedded in shape functions of the wavelet Galerkin method. Note that these coarsened eigenfunctions cannot be

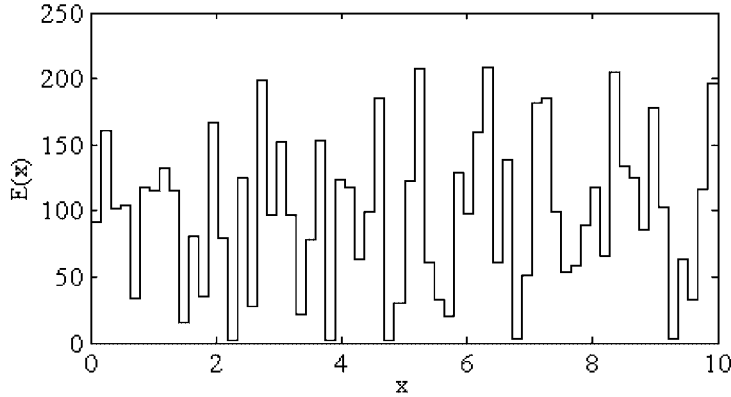


Figure 7. Highly oscillatory coefficient $E(x)$.

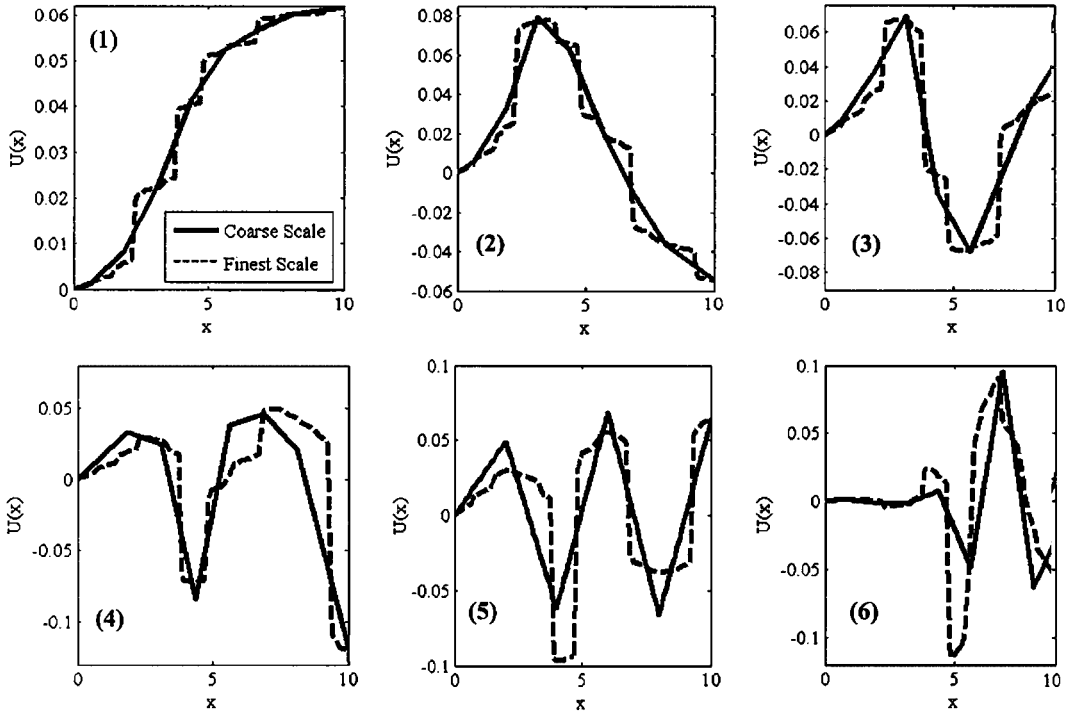


Figure 8. Wavelet Galerkin solution of eigenvalue problems $(E(x)u'(x))' + \beta u(x) = 0, u(0) = u'(0) = 0$: first six eigenfunctions at the finest scale ($j=9$) and coarse scale ($j=3$).

obtained accurately simply by projecting the finest eigenfunctions to the lower scales by wavelet projection method [11] as illustrated in Figure 9. It is shown that the wavelet projection of eigenfunctions improperly smears out fine certain scale characteristics.

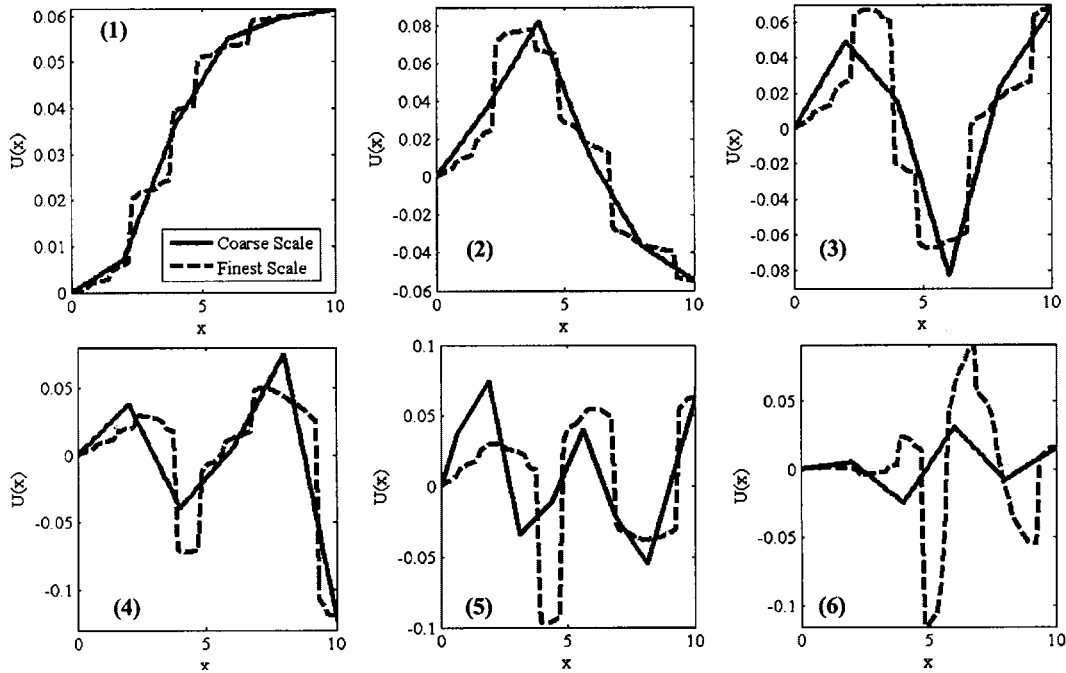


Figure 9. Wavelet projection of finest-scale eigenfunction of $(E(x)u'(x))' + \beta u(x) = 0$, $u(0) = u'(0) = 0$: first six projected eigenfunctions at the finest scale ($j=9$) and coarse scale ($j=3$).

5.3. Two-dimensional multi-scale homogenization

Consider the following Laplace equation

$$\nabla \cdot (E(x, y)\nabla u(x, y)) = 0, \quad 0 \leq x, y \leq 1 \quad (51)$$

$$u(1, y) = u(x, 1) = 10 \quad (52)$$

$$u(0, 0) = 5$$

with highly oscillatory coefficients $E(x, y)$ shown in Figure 10. 2D bilinear orthogonal scaling function and wavelet illustrated in Figures 2(a)–(d) and wavelet decomposition algorithm in Equation (B3) are utilized to construct the discrete equation in multi-scale homogenization. To capture the finest details of the solution, homogenization process starts from the finest scale $j=5$. Note that the mirror image method is also employed to preserve boundary conditions during homogenization processes. The homogenized solutions at multiple scales are shown in Figure 11, where the oscillatory part of the solution is filtered out in multi-scale homogenization.

6. CONCLUSION

A multi-scale wavelet Galerkin homogenization method has been proposed for the homogenization of heterogeneous materials. This approach removes some limitations of asymptotic method

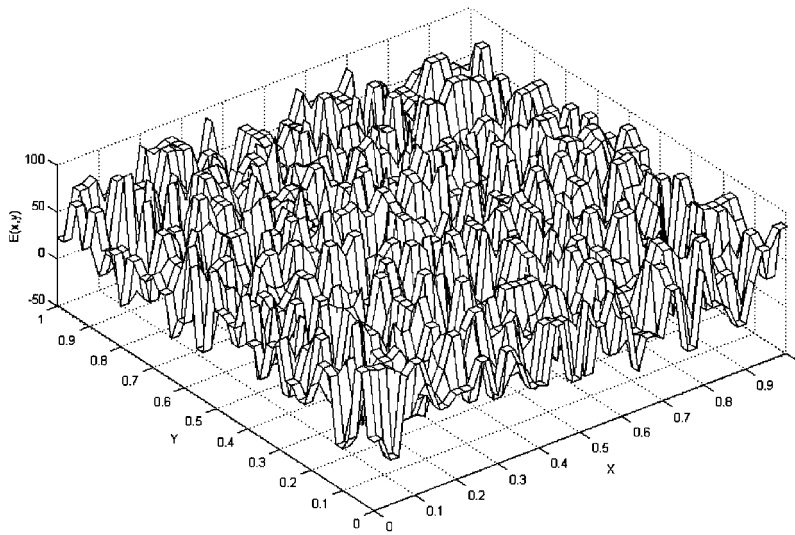


Figure 10. Highly oscillatory coefficient $E(x, y)$.

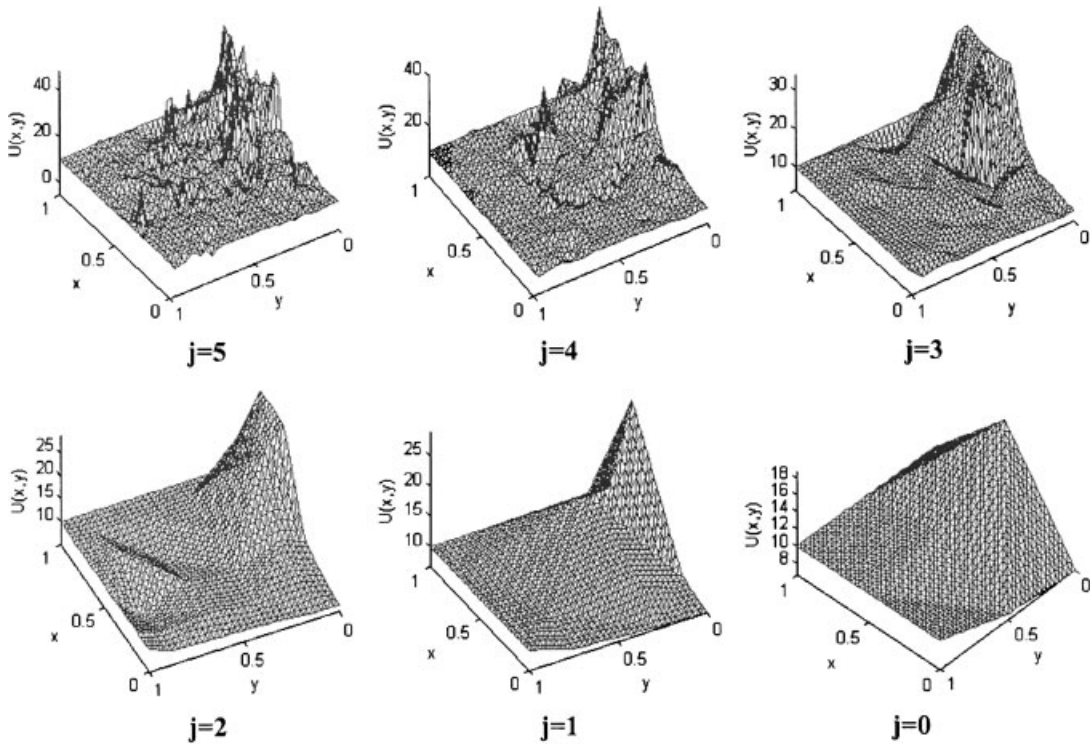


Figure 11. Two-dimensional multi-scale wavelet Galerkin homogenization solution.

in homogenization. The main features of the proposed method are:

- No restriction on periodicity of microscale structure.
- Discrete differential operator at any scale level can be obtained.
- Fast zoom-in and zoom-out capabilities.
- High-scale components of the solution (wavelet residual) can be used as an indicator for adaptive refinement.

In this work, the linear orthogonal scaling function and wavelet have been constructed and used as shape functions in the multi-scale wavelet Galerkin homogenization. Due to the dependency of the linear orthogonal scaling functions, the discrete differential operator (stiffness matrix) becomes singular when integration by parts is introduced in the Galerkin weak form. Using the transformation rules of the scaling functions and wavelets, the zero energy modes of the stiffness matrix have been analytically obtained. It has been shown that the linear combination of local zero energy modes yields five communicable global zero energy modes, and their explicit expressions have been derived. With the analytical forms of the global zero energy modes, the singularity of the stiffness matrix can be removed by an eigenvalue shifting approach.

Since the finest scale discrete equation was obtained via wavelet Galerkin method with scaling functions used as the shape functions, the present approach allows the discrete differential operator be obtained at any scale. This offers the opportunities of applying the proposed method to multi-scale problems where the multi-scale discrete operators are needed. An example is the eigenvalue analysis of multi-scale problems, where the multi-scale modes are obtained using the multi-scale stiffness matrices. In this case it can be shown that the eigenmodes of a specific scale obtained simply by a wavelet projection [11] of the finest scale modes do not satisfy the eigenvalue equation at that scale. In this case the multi-scale stiffness matrices are needed to obtain correct multi-scale eigenfunctions.

APPENDIX A: SCALE DECOMPOSITION COEFFICIENTS OF LINEAR ORTHOGONAL SCALING FUNCTIONS AND WAVELETS

Scale decomposition coefficients of linear orthogonal scaling functions and wavelets are tabulated in Table AI.

APPENDIX B: DISCRETIZED COARSE AND FINE SCALE SOLUTION COMPONENTS, DECOMPOSITION AND RECONSTRUCTION ALGORITHMS IN TWO DIMENSION

Applying wavelet decomposition to discretize the coarse and fine scale components of the solution yields

$$\begin{aligned}\bar{u}^j(x, y) &= \sum_m \sum_n \bar{u}_{m,n}^j \phi_{m,n}^j(x, y) \\ \tilde{u}^j(x, y) &= \sum_m \sum_n \tilde{u}_{m,n}^{\alpha j} \alpha_{m,n}^j(x, y) + \sum_m \sum_n \tilde{u}_{m,n}^{\beta j} \beta_{m,n}^j(x, y) + \sum_m \sum_n \tilde{u}_{m,n}^{\psi j} \psi_{m,n}^j(x, y)\end{aligned}\tag{B1}$$

Table AI. Decomposition coefficients ($a_n = a_{-n}$, $b_n = b_{-n-2}$).

n	a_n	n	b_n
0	0.817646595961945	-1	0.817646595961945
1	0.397296919701700	0	-0.397296919701700
2	-0.069101397548309	1	-0.069101397548309
3	-0.051944587049999	2	0.051944587049999
4	0.016972531859965	3	0.016972531859965
5	0.009987734381633	4	-0.009987734381633
6	-0.003888792672210	5	-0.003888792672210
7	-0.002191236880415	6	0.002191236880415
8	0.000944025366123	7	0.000944025366123
9	0.000473612955027	8	-0.000473612955027
10	-0.000315829481785	9	-0.000315829481785
11	-0.000036249000464	10	0.000036249000464

where

$$\begin{aligned}
 \phi_{m,n}^j(x, y) &= \phi_{j,m}^*(x)\phi_{j,n}^*(y) \\
 \alpha_{m,n}^j(x, y) &= \phi_{j,m}^*(x)\psi_{j,n}^*(y) \\
 \beta_{m,n}^j(x, y) &= \psi_{j,m}^*(x)\phi_{j,n}^*(y) \\
 \psi_{m,n}^j(x, y) &= \psi_{j,m}^*(x)\psi_{j,n}^*(y)
 \end{aligned}
 \tag{B2}$$

With above definition of 2D scaling function and wavelets, the 2D decomposition (fine to coarse) relationship can be obtained following Equation (15). Hence, the decomposition of coarse scale solution at scale $j + 1$ to coarse and fine scale solutions at scale j can be obtained by

$$\begin{aligned}
 \bar{u}_{k,l}^j &= 2 \sum_m \sum_n a_{m-2k} a_{n-2l} \bar{u}_{k,l}^{j+1} \\
 \tilde{u}_{k,l}^{\alpha j} &= 2 \sum_m \sum_n a_{m-2k} b_{n-2l} \tilde{u}_{k,l}^{\alpha(j+1)} \\
 \tilde{u}_{k,l}^{\beta j} &= 2 \sum_m \sum_n b_{m-2k} a_{n-2l} \tilde{u}_{k,l}^{\beta(j+1)} \\
 \tilde{u}_{k,l}^{\psi j} &= 2 \sum_m \sum_n b_{m-2k} b_{n-2l} \tilde{u}_{k,l}^{\psi(j+1)}
 \end{aligned}
 \tag{B3}$$

By following Equation (17), coarse scale solution at scale $j + 1$ can be reconstructed from coarse and fine scale solution at scale j by

$$\begin{aligned}
 \bar{u}_{k,l}^{j+1}(x, y) &= (1/2) \sum_m \sum_n r_{k-2m} r_{l-2n} \bar{u}_{m,n}^j + (1/2) \sum_m \sum_n r_{k-2m} s_{l-2n} \tilde{u}_{m,n}^{\alpha j} \\
 &+ (1/2) \sum_m \sum_n s_{k-2m} r_{l-2n} \tilde{u}_{m,n}^{\beta j} + (1/2) \sum_m \sum_n s_{k-2m} s_{l-2n} \tilde{u}_{m,n}^{\psi j}
 \end{aligned}
 \tag{B4}$$

APPENDIX C: DATA COMPACTNESS AND MIRROR IMAGE TECHNIQUE

As shown in Figure C1, at the coarser levels we have less data points with respect to the finer levels. This is due to the fact that information at each coarse scale node is provided by some adjacent nodes at the finer scale. As a consequence, the coarse levels data is only available at the nodes toward the centre of the domain. If no information is provided for the points outside the domain, the zero coefficients associated with the representative data points outside the domain of response will pollute the whole solution after a few steps of the homogenization process. The proposed remedy for this problem is a mirror image technique [10], by extending the physical domain with solution data to a fictitious domain with anti-symmetric data as shown in Figure C2. In this case, the average of solution at boundaries remains unchanged. Hence, this process does not generate any projection onto the wavelet spaces, since the wavelet projection filters out the deviation from the average.

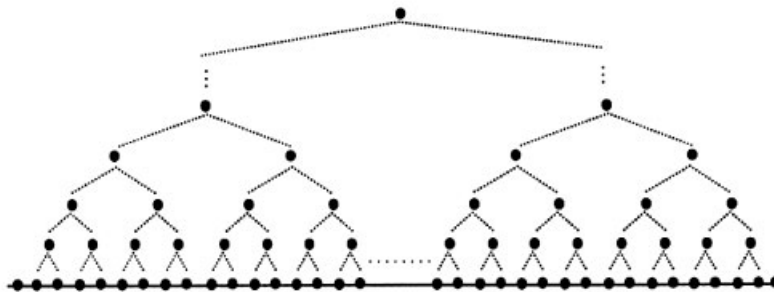


Figure C1. Data compactness through the reduction process of wavelet-based homogenization.

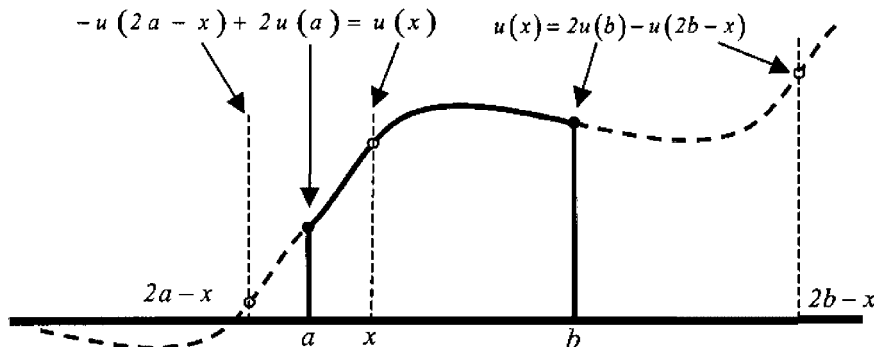


Figure C2. Mirror image data construction in the fictitious domain (a and b : boundaries of real domain).

ACKNOWLEDGEMENT

The support of this work by NSF under Grant CMS 0084589 to University of California, Los Angeles is greatly acknowledged.

REFERENCES

1. Bensoussan A, Lions JL, Papanicolaou G. *Asymptotic Analysis for Periodic Structures*. Elsevier: Amsterdam, 1978.
2. Oden JT, Zohdi TI. Analysis and adaptive modeling of highly heterogeneous elastic structures. *Computer Methods in Applied Mechanics and Engineering* 1997; **148**:367–391.
3. Oden JT, Vemaganti K, Moes N. Hierarchical modeling of heterogeneous solids. *Computer Methods in Applied Mechanics and Engineering* 1999; **172**:3–25.
4. Knappek S. Matrix-dependent multi-grid homogenization for diffusion problems. *SIAM Journal on Scientific Computing* 1996; **20**:515–533.
5. Fish J, Belsky V. Multigrid method for periodic heterogeneous media, 1-Convergence studies for one-dimensional media. *Computer Methods in Applied Mechanics and Engineering* 1995; **126**(1):1–16.
6. Brewster M, Beylkin G. A multiresolution strategy for numerical homogenization. *Applied and Computational Harmonic Analysis* 1995; **2**:327–349.
7. Dorobantu M, Engquist B. Wavelet-based numerical homogenization. *SIAM Journal on Numerical Analysis* 1998; **35**(2):540–559.
8. Coult NA. A multiresolution strategy for homogenization of partial differential equations. *Ph.D. Thesis*, Department of Applied Mathematics, University of Colorado, 1997.
9. Liu WK, Chen Y, Uras RA, Chang CT. Generalized multiple scale reproducing kernel particle methods. *Computer Methods in Applied Mechanics and Engineering* 1996; **139**:91–158.
10. Liu WK, Hao W, Chen Y, Jun S, Gosz J. Multiresolution reproducing kernel particle methods. *Computational Mechanics* 1997; **20**(4):295–309.
11. Mehraeen S, Chen JS. Wavelet-based multi-scale projection method in homogenization of heterogeneous media. *Finite Elements in Analysis and Design* 2004; **40**:1665–1679.
12. William JR, Amaratunga K. Introduction to wavelets in engineering. *International Journal for Numerical Methods in Engineering* 1994; **37**:2365–2388.
13. Qian S, Weiss J. Wavelets and the numerical solution of partial differential equations. *Journal of Computational Physics* 1993; **106**(1):155–175.
14. Dahlke S, Weinreich I. Wavelet Galerkin methods: an adapted biorthogonal wavelet basis. *Constructive Approximation* 1993; **9**:237–262.
15. Amaratunga K, William J, Yokoyama S. Wavelet-based hierarchical solutions of partial differential equations. *Proceeding of Third International Conference on Computational Plasticity, Fundamentals and Applications*. Barcelona, 1992.
16. Weiss J. Wavelet and the study of two dimensional turbulence. *Proceeding of French–U.S.A. Workshop on Wavelets and Turbulence*. Springer: New York, 1991.
17. Latto A, Resnikoff H, Tenenbaum E. The evaluation of the connection coefficients of compactly supported wavelets. *Proceeding of French–U.S.A. Workshop on Wavelets and Turbulence*. Springer: New York, 1992.
18. Chui CK. *An Introduction to Wavelets*. Academic Press: New York, 1992.
19. Chen JS, Pan C, Chang TYP. On the control of pressure oscillation in bilinear-displacement constant-pressure element. *Computer Methods in Applied Mechanics and Engineering* 1995; **128**:137–152.
20. Christon MA, Roach DW. The numerical performance of wavelets for PDEs: the multi-scale finite element. *Computational Mechanics* 2000; **24**:230–244.